

Recent results of the ISOFAZIA experiment

S. PIANTELLI⁽¹⁾, G. PASTORE⁽¹⁾⁽²⁾, R. ALBA⁽⁸⁾, S. BARLINI⁽¹⁾⁽²⁾, M. BINI⁽¹⁾⁽²⁾,
E. BONNET⁽¹³⁾, B. BORDERIE⁽¹¹⁾, R. BOUGAULT⁽⁵⁾, M. BRUNO⁽³⁾⁽⁴⁾,
A. BUCCOLA⁽¹⁾⁽²⁾, A. CAMAIANI⁽¹⁾⁽²⁾, G. CASINI⁽¹⁾, A. CHBIHI⁽¹²⁾,
C. CIAMPI⁽¹⁾⁽²⁾, M. CICERCHIA⁽⁶⁾⁽¹⁵⁾, M. CINAUSERO⁽⁶⁾, D. DELL'AQUILA⁽⁷⁾,
J. A. DUEÑAS⁽¹⁸⁾, D. FABRIS⁽⁹⁾, L. FRANCALANZA⁽¹⁴⁾, J. D. FRANKLAND⁽¹²⁾,
C. FROSIN⁽¹⁾⁽²⁾, F. GRAMEGNA⁽⁶⁾, D. GRUYER⁽⁵⁾, M. HENRI⁽⁵⁾, A. KORDYASZ⁽¹⁶⁾,
T. KOZIK⁽¹⁷⁾, N. LE NEINDRE⁽⁵⁾, I. LOMBARDO⁽¹⁰⁾, O. LOPEZ⁽⁵⁾, C. MAIOLINO⁽⁸⁾,
G. MANTOVANI⁽⁶⁾⁽¹⁵⁾, T. MARCHI⁽⁶⁾, L. MORELLI^{(3)(4)(*)}, A. OLMI⁽¹⁾⁽²⁾,
P. OTTANELLI⁽¹⁾⁽²⁾, M. PARLOG⁽⁵⁾⁽¹⁹⁾, G. PASQUALI⁽¹⁾⁽²⁾, G. POGGI⁽¹⁾⁽²⁾,
D. SANTONOCITO⁽⁸⁾, A. A. STEFANINI⁽¹⁾⁽²⁾, S. VALDRÉ⁽¹⁾, G. VERDE⁽¹⁰⁾,
E. VIENT⁽⁵⁾ and M. VIGILANTE⁽¹⁴⁾

⁽¹⁾ INFN, Sezione di Firenze - Firenze, Italy

⁽²⁾ Dipartimento di Fisica, Università di Firenze - Firenze, Italy

⁽³⁾ Dipartimento di Fisica, Università di Bologna - Bologna, Italy

⁽⁴⁾ INFN, Sezione di Bologna - Bologna, Italy

⁽⁵⁾ Normandie Université, ENSICAEN, UNICAEN, CNRS/IN2P3, LPC Caen - F-14000 Caen, France

⁽⁶⁾ INFN, Laboratori Nazionali di Legnaro - Legnaro (PD), Italy

⁽⁷⁾ National Superconducting Cyclotron Laboratory, Michigan State University - East Lansing, MI 48824, USA

⁽⁸⁾ INFN, Laboratori Nazionali del Sud - Catania, Italy

⁽⁹⁾ INFN, Sezione di Padova - Padova, Italy

⁽¹⁰⁾ INFN, Sezione di Catania - Catania, Italy

⁽¹¹⁾ IPN, CNRS/IN2P3, Univ. Paris-Sud, Université Paris-Saclay - F-91406 Orsay cedex, France

⁽¹²⁾ GANIL, CEA/DRFCNRS/IN2P3 - Bvd. Henri Becquerel, 14076 Caen, France

⁽¹³⁾ SUBATECH UMR 6457, IMT Atlantique, Université de Nantes, CNRS-IN2P3 - 44300 Nantes, France

⁽¹⁴⁾ Dipartimento di Fisica "E. Pancini" and Sezione INFN, Università di Napoli "Federico II" - I-80126 Napoli, Italy

⁽¹⁵⁾ Dipartimento di Fisica, Università di Padova - Padova, Italy

⁽¹⁶⁾ Heavy Ion Laboratory, Warsaw University - Warsaw, Poland

⁽¹⁷⁾ Jagiellonian University - Cracow, Poland

⁽¹⁸⁾ Departamento de Ingeniería Eléctrica y Centro de Estudios Avanzados en Física, Matemáticas y Computación, Universidad de Huelva - 21071 Huelva, Spain

⁽¹⁹⁾ "Horia Hulubei" National Institute for R&D in Physics and Nuclear Engineering (IFIN-HH) - P.O.BOX MG-6, Bucharest Măgurele, Romania

received 3 December 2018

(*) Present address: GANIL, CEA/DRFCNRS/IN2P3, Bvd. Henri Becquerel, 14076 Caen, France

Summary. — Recent results concerning isospin transport phenomena on the systems $^{80}\text{Kr} + ^{40,48}\text{Ca}$ at 35 MeV/nucleon are presented. An investigation of the isospin content of both fission fragments coming from the QuasiProjectile is also shown. Data were collected with four FAZIA blocks (ISOFAZIA experiment). A comparison with the predictions of a transport model (AMD) is also reported.

1. – The experiment

ISOFAZIA was the first physics experiment performed by the FAZIA Collaboration after the R&D phase [1]. A ^{80}Kr beam ($N/Z = 1.22$) at 35 MeV/nucleon, delivered by the superconducting cyclotron CS of INFN-LNS (Catania, Italy), and two different targets, a neutron-rich ^{48}Ca ($N/Z = 1.40$) and a neutron-poor ^{40}Ca ($N/Z = 1.00$) were used, in such a way that the N/Z of the projectile was intermediate between those of both targets. The experimental setup consisted of 4 complete blocks, each one including 16 silicon (thickness: 300 μm) - silicon (thickness: 500 μm) - CsI (thickness: 10 cm, read out by a photodiode) telescopes, located in a belt configuration, covering the polar angles in the range 2.3° – 16.6° and symmetrically located with respect to the beam axis.

2. – Event sorting

The collected events were sorted in two classes on the basis of the correlation Z_{TOT} *vs.* ϑ_{flow}^{cm} , where Z_{TOT} is the total detected charge and ϑ_{flow}^{cm} is the c.m. flow angle built including all the detected products coming from various reactions: incomplete fusion or multifragmentation reactions on the one side ($50^\circ \leq \vartheta_{flow}^{cm}$) and Deep Inelastic Collision (DIC) type on the other ($8^\circ \leq \vartheta_{flow}^{cm} \leq 30^\circ$). More details on the adopted selections are reported in [2].

Among the events belonging to the DIC class those with two fragments were further separated in QP-QT (QuasiProjectile-QuasiTarget) events and QP fission events by means of the correlation ϑ_{rel}^{cm} (relative angle in the centre of mass between the two fragments) *vs.* v_{rel} (relative velocity), as shown in fig. 1 (left side for the experimental data), where the two classes are identified by black and red rectangles, respectively.

The adopted selections were checked by means of a simulation based on the AMD code [3, 4] followed by GEMINI++ [5] as afterburner. The dynamical calculation was stopped at 500 fm/c; a stiff ($L = 108$ MeV) and a soft ($L = 46$ MeV) parametrizations [4] of the symmetry energy term of the nuclear equation of state were tested. In order to take into account the geometrical coverage of the setup and the identification thresholds, a software replica of the setup was applied to the simulated data before comparing them to the experimental results.

The simulation proved to be able to reproduce in a reasonable way the main features of the reactions over the entire impact parameter range. For example, in the right part of fig. 1 the simulated correlation between ϑ_{rel}^{cm} and v_{rel} for peripheral events with two fragments is shown, to be compared with the measured one (on the left). Besides, the average light fragment multiplicities detected in DIC events are quite well reproduced by the simulation, with the possible slight overestimation of $Z = 1$, as shown in fig. 2.

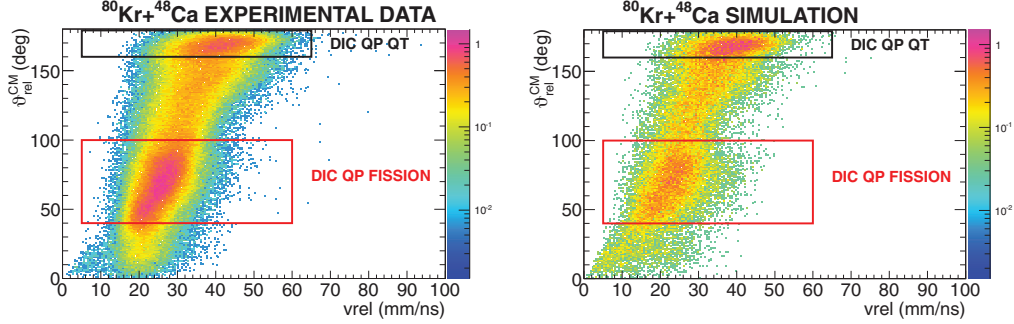


Fig. 1. $-\vartheta_{rel}^{cm}$ vs. v_{rel} correlation for the system $^{80}\text{Kr}+^{48}\text{Ca}$ at 35 MeV/nucleon. Left side: Experimental data. Right side: Simulated data (model: AMD with stiff parametrization followed by GEMINI++).

3. – Experimental results

Evidences of isospin diffusion [6-8] have been found looking at the $\langle N \rangle / Z$ vs. Z distribution for the QP when the target changes from the n-poor ^{40}Ca to the n-rich ^{48}Ca , as shown in fig. 3 up to $Z = 25$ thanks to the excellent isotopic resolution of FAZIA. In particular, the $\langle N \rangle / Z$ of the QP is systematically higher when the target is the n-rich one. Similar results concerning the dependence of the isotopic composition of the QP on the neutron content of the target at lower beam energies have been shown for example in [9,10]. More indirect evidences, related to the emitted particles, can be found, for example, in [11-14].

For DIC events, the isotopic ratios of $Z = 1$ as a function of the parallel component of their centre of mass velocity with respect to the QP direction are shown in fig. 4 for the system $^{80}\text{Kr}+^{48}\text{Ca}$. Moving from the QP region towards the neck zone the isospin tends to increase both for the experimental data (full points; similar results can be found in many papers in the literature, see for example [15,16]) and for the simulation (squares). A weak indication towards a stiff symmetry energy emerges from these plots, because full squares are closer to the experimental data than open squares.

The same hint comes also from the first and second moments of the isotopic distribution of the IMF (Intermediate Mass Fragments) as a function of their charge, as

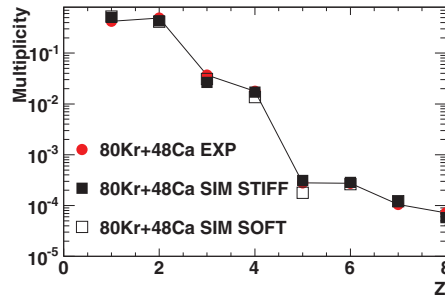


Fig. 2. – Light ejectile multiplicities detected in DIC events. Full circles: experimental data. Open squares: simulation with soft symmetry energy. Full squares: simulation with stiff symmetry energy.

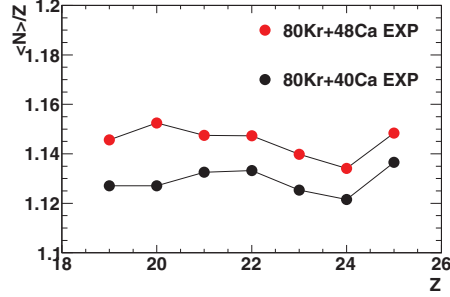


Fig. 3. – $\langle N \rangle / Z$ vs. Z for the QP. Full red circles: $^{80}\text{Kr}+^{48}\text{Ca}$ reaction. Full black circles: $^{80}\text{Kr}+^{40}\text{Ca}$ reaction.

shown in fig. 5, where full squares (corresponding to the stiff simulation) better follow the experimental trend.

Concerning the QP fission, in the experimental data set there is a prevalence of asymmetric splittings, as shown in fig. 6, left side, where the correlation between the charge of the two fragments is shown. The asymmetry η is calculated in terms of charge of the fragments as $\eta = \frac{Z_{big} - Z_{small}}{Z_{big} + Z_{small}}$, where $Z_{big}(small)$ is the charge of the biggest (smallest) fragment of the couple. Referring to the α angle as done in [17], defined as the angle between the QP splitting axis and the QP-QT separation axis, it is interesting to investigate the dependence of the $\cos \alpha$ distribution on η , as shown in fig. 6, right side. From the picture it clearly emerges that symmetric break-ups present a rather flat $\cos \alpha$ distribution, while the more asymmetric the fission the more forward peaked the $\cos \alpha$ distribution. $\cos \alpha = 1$ corresponds to collinear splits, with the smaller fragment emitted towards the QT. In the hypothesis that the α angle is correlated to the splitting time [17] (the faster the splitting the smaller the α angle, because the QP has a shorter time to rotate before fissioning), this plot says that asymmetric fissions tend to be fast and aligned, with the smaller fragment emitted towards the QT, as found also in [13, 18].

According to a well-known scenario emerging from transport models, the isospin drift mechanism [6, 7] generates a neutron enrichment in the neck zone; as a consequence, the part of the QP closer to the neck region should be more neutron rich than the

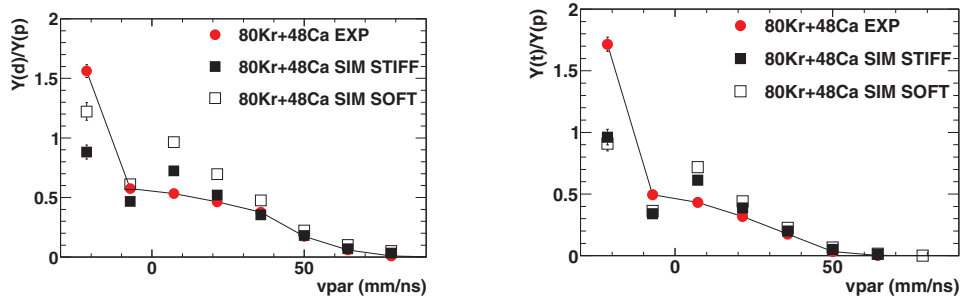


Fig. 4. – Left: d/p multiplicity ratio as a function of the parallel component of the centre-of-mass velocity of the LCP with respect to the QP direction. Right: the same for t/p. Data refer to $^{80}\text{Kr}+^{48}\text{Ca}$. Full circles: experimental data. Squares: simulation with stiff (full) and soft (open) parametrization.

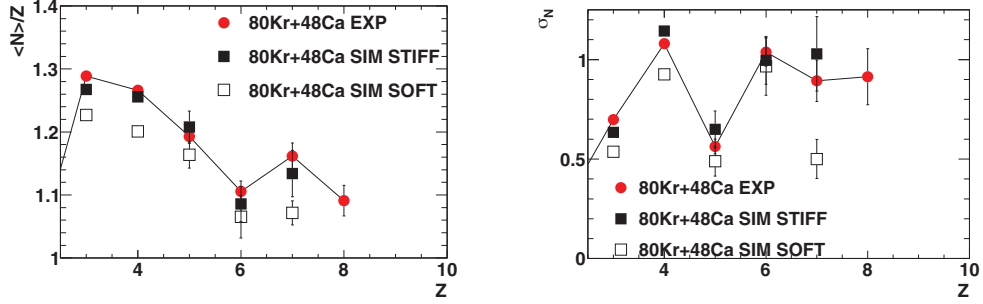


Fig. 5. – First (left) and second (right) moment of the IMF isotopic distribution *vs.* the IMF charge. Data refer to $^{80}\text{Kr}+^{48}\text{Ca}$. Full circles: experimental data. Squares: simulation with asystiff (full) and asysoft (open) parametrization.

remaining part of the fragment. If the QP fissions on long time scale, the isospin degree of freedom has enough time to equilibrate before the splitting. On the contrary if the fission process is fast, the two fission fragments have not enough time to completely equilibrate their isospin, with the degree of equilibration depending on the splitting time. This effect can be put in evidence looking at the average isospin of the big and the small fission fragments as a function of the α angle and for different η windows, as done in [17, 19]. At small η values (left side of fig. 7) the big (full red squares) and the small (full red circles) fission fragments have the same average isospin asymmetry (measured as $\Delta = \langle \frac{N-Z}{A} \rangle$ [17]), independently of α . Therefore symmetric breakups should correspond to slow timescales, as evidenced also from the flat distribution of $\cos \alpha$ (right side of fig. 6). On the contrary, at larger η , (right side of fig. 7), when α is small (*i.e.*, when the fission is fast), a wide difference in the isospin of the two fragments is observed, with the smaller one more neutron rich than the bigger one. Such difference tends to decrease with increasing α , *i.e.*, when the slower fission dynamics allows the two fission partners to reach an isospin equilibration. The observed trend, which is consistent with the results presented in [17, 19], is also qualitatively reproduced by the model (full and open black symbols in fig. 7), although the latter systematically underestimates the values of Δ .

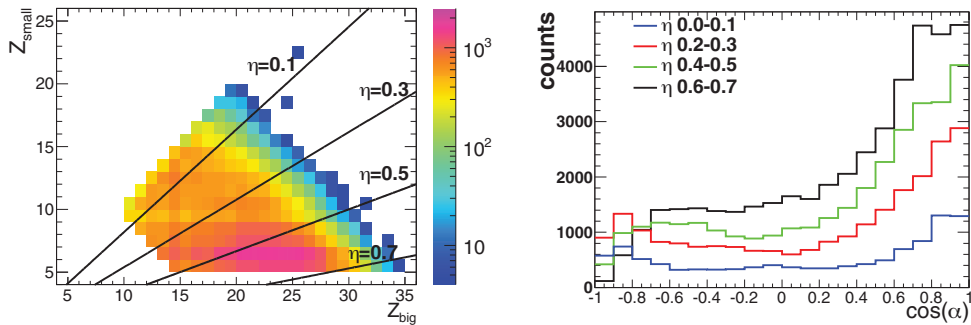


Fig. 6. – Experimental data for the system $^{80}\text{Kr}+^{48}\text{Ca}$. Left: charge correlation between the two fission fragments coming from the QP. Lines corresponding to different η windows are shown. Right: $\cos \alpha$ distribution for different η windows.

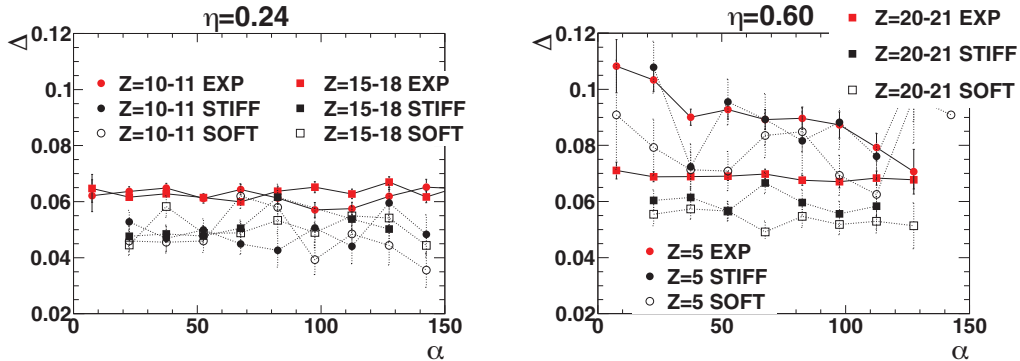


Fig. 7. – $\Delta = \langle \frac{N-Z}{A} \rangle$ as a function of α for $\eta = 0.24$ (left) and $\eta = 0.60$ (right). Red symbols: experimental data for the reaction $^{80}\text{Kr}+^{48}\text{Ca}$. Full black symbols: simulation with stiff parametrization. Open black symbols: simulation with soft parametrization.

4. – Summary and conclusions

Some experimental findings concerning the systems $^{80}\text{Kr}+^{48,40}\text{Ca}$ at 35 MeV/nucleon have been discussed. Data were collected by the FAZIA Collaboration in the first physics experiment (ISOFAZIA) after the R&D phase, with a limited setup (four complete blocks). Semiperipheral collisions have been selected, checking the validity of the applied criteria by means of a simulation based on the AMD code followed by GEMINI++ as afterburner. A first noticeable result is the capability of the simulation to nicely reproduce most features of these collisions. Within this model two different recipes for the symmetry energy term of the nuclear equation of state were tested, finding a weak indication towards a stiff term by considering the isotopic composition of light charged particles and light fragments. Concerning the QP fission, indications that fast splitting is favoured for asymmetric break-up have been found, looking at the $\cos\alpha$ distribution for different η windows. For the same class of events (large η) a wide isospin asymmetry between the small and the big fragment is observed when α is small, with the gap decreasing with increasing α . According to [17] this could be interpreted as the result of a trend towards isospin equilibration between the fission fragments for slower splittings. The observed trend is qualitatively reproduced by the adopted model.

A better investigation of these phenomena will be pursued in the next years when the FAZIA (12 blocks) plus INDRA [20] setup starts the data taking, thanks to the improved angular coverage. Anyway, some useful information on the QP fission process might come also from dedicated experiments with a reduced FAZIA setup at forward angles and other devices such as OSCAR [21] at backward angles in order to detect the QT, for a better selection and characterization of binary events, also in terms of the centrality.

* * *

We would like to thank both the GARR Consortium for the kind use of the computing resources on the platform cloud.garr.it and the INFN-CNAF for the use of the cloud infrastructure.

REFERENCES

- [1] BOUGAULT R. *et al.*, *Eur. Phys. J. A*, **50** (2014) 1.
- [2] PASTORE G., PhD Thesis, Università di Firenze (2017).
- [3] ONO A., *Phys. Rev. C*, **59** (1999) 853.
- [4] ONO A., *J. Phys. Conf. Ser.*, **420** (2013) 012103.
- [5] CHARITY R. J., *Phys. Rev. C*, **82** (2010) 014610.
- [6] NAPOLITANI P. *et al.*, *Phys. Rev. C*, **81** (2010) 044619.
- [7] BARAN V. *et al.*, *Phys. Rep.*, **410** (2005) 335.
- [8] TSANG M. B. *et al.*, *Phys. Rev. Lett.*, **92** (2004) 062701.
- [9] SOULIOTIS G. A. *et al.*, *Phys. Rev. C*, **84** (2011) 064607.
- [10] PIANTELLI S. *et al.*, *Phys. Rev. C*, **96** (2017) 034622.
- [11] LOMBARDO I. *et al.*, *Phys. Rev. C*, **82** (2010) 014608.
- [12] GALICHET E. *et al.*, *Phys. Rev. C*, **79** (2009) 064614.
- [13] DEFILIPPO E. *et al.*, *Phys. Rev. C*, **86** (2012) 014610.
- [14] BARLINI S. *et al.*, *Phys. Rev. C*, **87** (2013) 054607.
- [15] PIANTELLI S. *et al.*, *Phys. Rev. C*, **74** (2006) 034609.
- [16] BOUGAULT R. *et al.*, *Phys. Rev. C*, **97** (2018) 024612.
- [17] JEDELE A. *et al.*, *Phys. Rev. Lett.*, **118** (2017) 062501.
- [18] CASINI G. *et al.*, *Phys. Rev. Lett.*, **71** (1993) 2567.
- [19] RODRIGUEZ MANSO A. *et al.*, *Phys. Rev. C*, **95** (2017) 044604.
- [20] POUTHAS J. *et al.*, *Nucl. Instrum. Methods A*, **357** (1995) 418.
- [21] DELL'AQUILA D. *et al.*, *Nucl. Instrum. Methods A*, **877** (2018) 227.